

Underfrequency Load Shedding for an Islanded Distribution System With Distributed Generators

Pukar Mahat, *Student Member, IEEE*, Zhe Chen, *Senior Member, IEEE*, and Birgitte Bak-Jensen, *Member, IEEE*

Abstract—Significant penetration of distributed generation in many distribution systems has opened an option of operating distribution systems in island mode for economical and technical reasons. However, balancing frequency of the islanded system is still an issue to be solved, especially when the demand exceeds the generation in the power island. This paper presents a strategy to shed an optimal number of loads in the island to stabilize the frequency. The load shedding strategy is based on frequency information, rate of change of frequency, customers' willingness to pay, and loads histories. Different scenarios have been simulated with results showing that the proposed method is effective in shedding the optimal number of loads while stabilizing frequency.

Index Terms—Distributed generation (DG), islanding, rate of change of frequency, underfrequency load shedding, willingness to pay (WTP).

I. INTRODUCTION

HERE is global interest in distributed generation (DG) as a replacement to the centralized power plants. There are, however, various technical and economical challenges to bring this technology into the mainstream of a power market largely dominated by large centralized plants. Despite this, many electricity markets in Europe have been able to integrate a large number of wind turbines (WTs) and small district combined heat and power plants (DCHP) into the system [1]. It is expected to increase further with people's propensity for renewable energy. DGs currently operate together with the grid with utilities requiring that DGs be disconnected from the grid as soon as possible in the event of islanding, a situation in which the distributed system becomes electrically isolated from the remainder of the power system, yet continues to be energized by the DGs connected to it. IEEE 929-1988 Std. [2] requires the disconnection of DGs once they are islanded. IEEE 1547-2003 Std. [3] stipulates a maximum delay of 2 s for the detection of an unintentional island and for all DGs to cease energizing the distribution system. But with the increasing number of DGs on distribution systems, it may not be desirable to limit unintentional islanding.

The current practice of disconnecting the DGs following a disturbance will no longer be a practical or reliable solution in

the future. It is also expected that there will be increased competition among the energy suppliers to secure more customers by providing better power quality and reliability. Also, the IEEE Std. 1547-2003 [3] states that the implementation of intentional islanding of DGs is one of its tasks for future consideration. Thus, island operation of DG is a viable option.

When the distributed system with DG is islanded, most often the frequency will change. The frequency will either go up if there is excess generation or down if there is excess load. If the frequency goes up, it can be controlled by reducing the output power of the generators. Photovoltaic generators use maximum power point tracking, variable speed wind turbines optimize power coefficient (C_p) to produce maximum power, and DCHPs operate at maximum power. Thus, if all of the generators are operating at maximum power and the frequency goes down, some loads have to be shed to bring the frequency back to normal.

The problem of optimal load shedding has been extensively investigated. A static load shedding strategy has been proposed in [4], which keeps on shedding a fixed amount of load with decreasing frequency. Fast-acting load shedding was proposed for implementation in the System Control Center in [5]. Supervisory-control and data-acquisition (SCADA)-based load shedding strategy has been proposed in [6]. Another load shedding scheme based upon SCADA for an isolated system is presented in [7]. And still another load shedding strategy based on the online measurement of the loads and load-frequency characteristics is presented in [8]. Loads with smaller frequency dependency are shed first and those with larger frequency dependency are shed later. The problem with these methods is that real-time information on loads is not always available and implementing online load measurement is expensive for small distribution systems. Furthermore, the system's load-frequency dependency is often hard to determine especially with constantly changing loads. There is also an adaptive load shedding strategy, which changes the relay settings according to the frequency decay curve [9] as well as a load shedding method based on the frequency information and integration of df/dt to find the amount of load to be shed [10]. Other adaptive load shedding strategies based on df/dt are presented in [11]–[15]. But the need for real-time load and generation data still persists. Furthermore, system inertia, which is needed to calculate the amount of load to be shed, is difficult to determine when the system has significant penetration of generations which are stochastic in nature, such as wind turbines or photovoltaic-powered generators. The load shedding strategy for the islanded distributed system should be treated differently from the large power system because of the differences in characteristics. Islanded distribution systems often have small generators and, hence, small inertia.

Manuscript received July 10, 2008; revised May 11, 2009. First published November 17, 2009; current version published March 24, 2010. This work was supported in part by PSO program, project 2006-1-6316, "Operation and Control of Modern Distribution Systems," in part by Himmerlands Elforsyning A.m.b.a, in part by SEAV-NVE, and in part by DEFU. Paper no. TPWRD-00544-2008.

The authors are with the Institute of Energy Technology, Aalborg University, Aalborg DK-9220, Denmark (e-mail: pma@iet.aau.dk; zch@iet.aau.dk; bbj@iet.aau.dk).

Digital Object Identifier 10.1109/TPWRD.2009.2032327

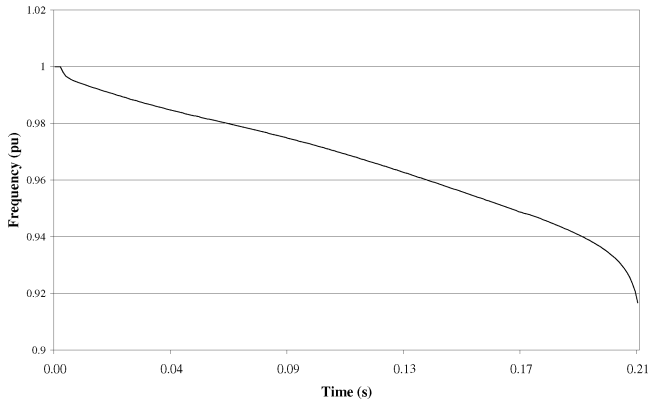


Fig. 1. System frequency after islanding.

Thus, the frequency tends to decay more rapidly as shown in Fig. 1. Furthermore, load shedding in the distribution system may not be governed by technical reasons alone but also economical reasons.

With the concept of custom power, customers will pay more for better power quality and reliability. A study in Sweden shows that the willingness to pay (WTP) is significantly higher for unplanned outages [16]. Distribution system operators are obligated to supply loads that are paying more without regard to demand size. The optimal load shedding strategy for an islanded distribution system, therefore, should shed the optimal number of loads. An underfrequency load shedding for islanded distribution systems with DGs based on frequency information, rate of change of frequency (RoCoF), customers' WTP, and loads histories is presented here. Loads histories can be easily obtained from data logs at load points. WTP can be determined by asking customers how much they are willing to pay for being supplied during islanding. This can be done at the same time when the customer chose the electricity tariff scheme. Ranking of load (NL) for load shedding is based on WTP. WTP is normalized with respect to the load that is willing to pay most for electricity.

The proposed methodology is explained in detail in Section II and it is tested in a radial distribution system, which is presented in Section III. The methodology is simulated in DigSILENT PowerFactory 13.2.334. Different scenarios have been simulated, and the results are presented in Section IV. Section V concludes this paper.

II. PROPOSED METHODOLOGY

The flowchart of the underfrequency load shedding scheme is shown in Fig. 2. Loads are ranked based on their willingness to pay. A lookup table is created and loads are shed according to it. It is created using the loads history and loads' willingness to pay. The procedure to construct lookup tables is described later.

Frequency is measured every half cycle and RoCoF is calculated. If RoCoF is negative, it might be necessary to shed some loads. If it is higher than $RoCoF_{LL}$, (RoCoF corresponding to lowest load), the methodology will wait for the frequency to go down below f_{LL} , (lower power quality limit of frequency), as the decay in frequency can be the result of some normal events

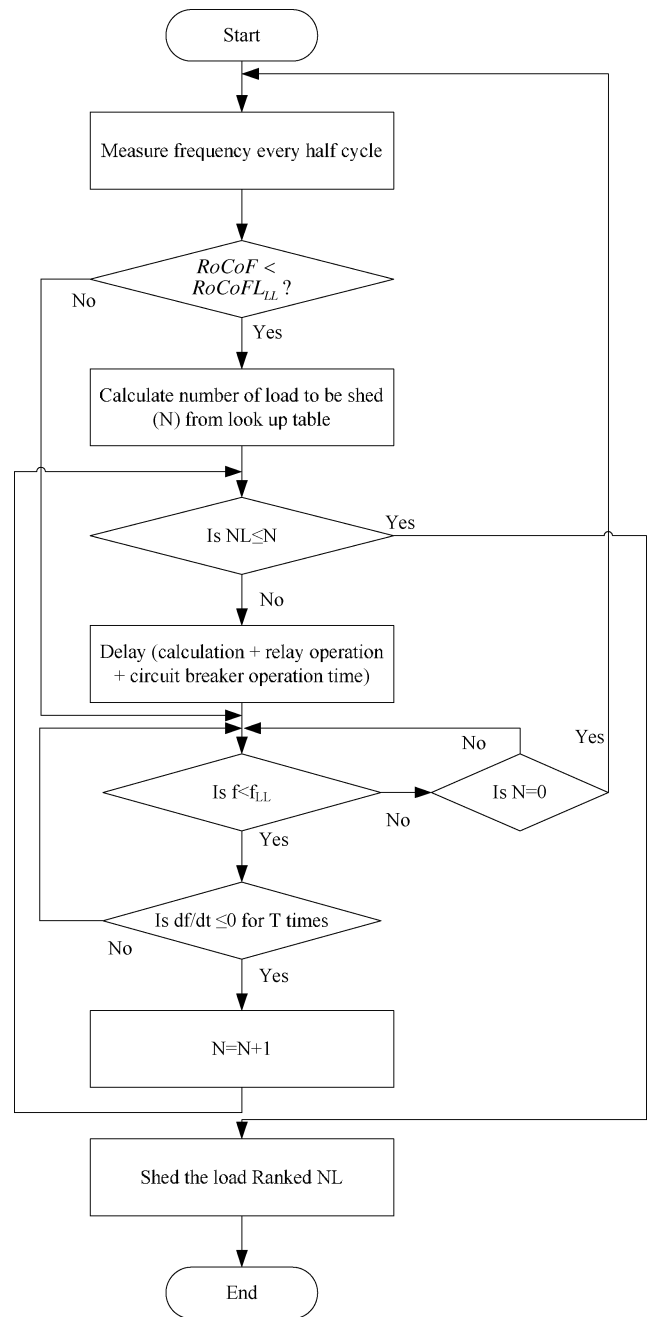


Fig. 2. Flowchart of the proposed methodology.

and the frequency might stabilize itself after some time. If the RoCoF is calculated to be lower than $RoCoF_{LL}$, some loads should be shed quickly as frequency tends to decay rapidly in a small system. The number of loads to be shed (N) is determined from the lookup table.

If the RoCoF calculated is between the corresponding $\sum_{i=1}^{NL} RoCoF_{L_i}$ of two loads, the NL corresponding to the load which has the lowest $\sum_{i=1}^{NL} RoCoF_{L_i}$ will be chosen as N . For example, if the RoCoF calculated is -30 Hz/s and loads ranked 3 and 4 have $\sum_{i=1}^{NL} RoCoF_{L_i}$ of -28 Hz/s and -35 Hz/s, respectively, then N is chosen as 4. The load shedding of N loads is initiated after the calculation of RoCoF and the determination of N from the lookup table. Ideally, the frequency

TABLE I
LOOKUP TABLE FOR THREE DIFFERENT CASES

Load Rank (NL)	Case 1 (Worst Case)				Case 2 (Random Case)				Case 3 (Best Case)			
	Load	WTP	RoCoFL _i	$\sum_{i=1}^{NL} RoCoFL_i$	Load	WTP	RoCoFL _i	$\sum_{i=1}^{NL} RoCoFL_i$	Load	WTP	RoCoFL _i	$\sum_{i=1}^{NL} RoCoFL_i$
1	Load 09	0.81	-15.66	-15.66	STSY	0.79	-53.23	-53.23	MAST	0.89	-69.86	-69.86
2	Load 10	0.83	-15.66	-31.31	Load 10	0.84	-15.66	-68.89	Load 07	0.9	-22.82	-92.69
3	Load 11	0.86	-15.66	-46.97	STNO	0.85	-48.36	-117.24	Load 09	0.91	-15.66	-108.34
4	Load 07	0.87	-22.82	-69.79	Load 09	0.86	-15.66	-132.90	Load 10	0.92	-15.66	-124.00
5	Load 08	0.89	-28.53	-98.33	STCE	0.89	-36.24	-169.15	STCE	0.93	-36.24	-160.25
6	JUEL	0.91	-30.63	-128.96	Load 07	0.9	-22.82	-191.97	STNO	0.94	-48.36	-208.60
7	STCE	0.92	-36.24	-165.21	Load 08	0.91	-28.53	-220.50	Load 11	0.95	-15.66	-224.26
8	FLØE	0.93	-48.36	-213.57	FLØE	0.95	-52.91	-273.41	JUEL	0.96	-30.63	-254.90
9	STSY	0.95	-52.91	-266.48	Load 11	0.98	-15.66	-289.07	FLØE	0.97	-52.91	-307.81
10	STNO	0.96	-53.23	-319.70	JUEL	0.99	-30.63	-319.70	Load 08	0.99	-28.53	-336.34
11	MAST	1	-69.86	-389.57	MAST	1	-69.86	-389.57	STSY	1	-53.23	-389.57

should come back to the normal operating range with the load shedding but sometimes some other loads should also be shed to bring the frequency back. This is because of the assumption made while forming the lookup table and it helps to shed an optimal number of loads. After the first step of load shedding is initiated, the loads will wait for some time before they will measure the frequency again. The delay will account for the calculations and circuit-breaker operation time. The unshed loads will have to wait for the frequency to go down below f_{LL} and for the RoCoF to be negative for “T” times before they are shed, provided that all of the loads ranked higher than them are already shed. The distribution system does not have the luxury of spinning reserve and secondary control like the transmission system. Thus, the only way to bring the frequency above the lower limit is to shed loads as its DGs are already operating at their maximum capacity. Waiting for the RoCoF to be negative for “T” half cycles will make sure the frequency is not coming back to nominal and frequency oscillation is accounted for. Choosing a longer “T” will result in the frequency reaching a lower value, especially when loads are highly frequency and voltage dependent, as enough loads are not shed in the first step. However, if smaller “T” is chosen, there is always a possibility of shedding more loads than required. Choosing T is system specific and depends on the preference between optimal load shedding and a better frequency profile. However, simulation results shows that choosing T around 10 can shed an optimal number of loads without letting the frequency to go down to a very low value even in worst-case scenarios.

A lookup table is created as follows by using the past information on loads and their willingness to pay.

- Step 1) Rank all of the loads with the load that is willing to pay the least ranked first and the load that is willing to pay the most ranked last.
- Step 2) Consider guaranteed generations only. Generation from sources, such as wind, solar, etc., may not be available all of the time.
- Step 3) Consider loads as constant PQ since dependency on frequency and voltage is difficult to determine.

- Step 4) Find the peak real power demand of individual loads for a previous period (P_{ppi}) from the data available.
- Step 5) Find the rate of change of frequency corresponding to a load ($RoCoFL_i$) by simulating an islanding with a system having a real power deficiency equivalent to (P_{ppi}). For example, if the previous peak real power demand of a load is 0.5 MW, then adjust loads in the system to make the real power deficiency in the system equivalent to 0.5 MW and calculate $RoCoFL_i$. With this, the load is assumed to be near 0.5 MW when the system is islanded in present time, and the frequency could be brought to normal by shedding the load should the RoCoF resulting from islanding be higher or equal to $RoCoFL_i$.
- Step 6) Repeat Step 5) for all of the loads.
- Step 7) Calculate $\sum_{i=1}^{NL} RoCoFL_i$ and create a lookup table like Table I. This gives a rough idea of how many loads should be shed to bring the frequency back to normal when the system is islanded.

By considering the peak demand of loads, guaranteed generations, and constant PQ, the RoCoF calculated will be lower compared to an actual case where loads might not be at peak or might have certain dependency on voltage and frequency or there might be some nonguaranteed generations. This will reduce the chance of shedding more loads than required.

III. TEST SYSTEM

Fig. 3 shows the system in which the proposed methodology is tested. The test system is a part of a distribution network, owned by Himmerlands Elforsyning, of Aalborg, Denmark. The test system consists of 11 loads, 3 fixed-speed stall-regulated wind turbine generators (WTGs) of 630 kW each and a combined heat and power (CHP) plant with 3 gas turbine generators of 3 MW each. Line data and generator data are given in [17]. The distribution system is connected to the transmission network at Bus 05. Islanding is simulated by opening the circuit breaker (CB). WTGs operate at unity power factor and so does

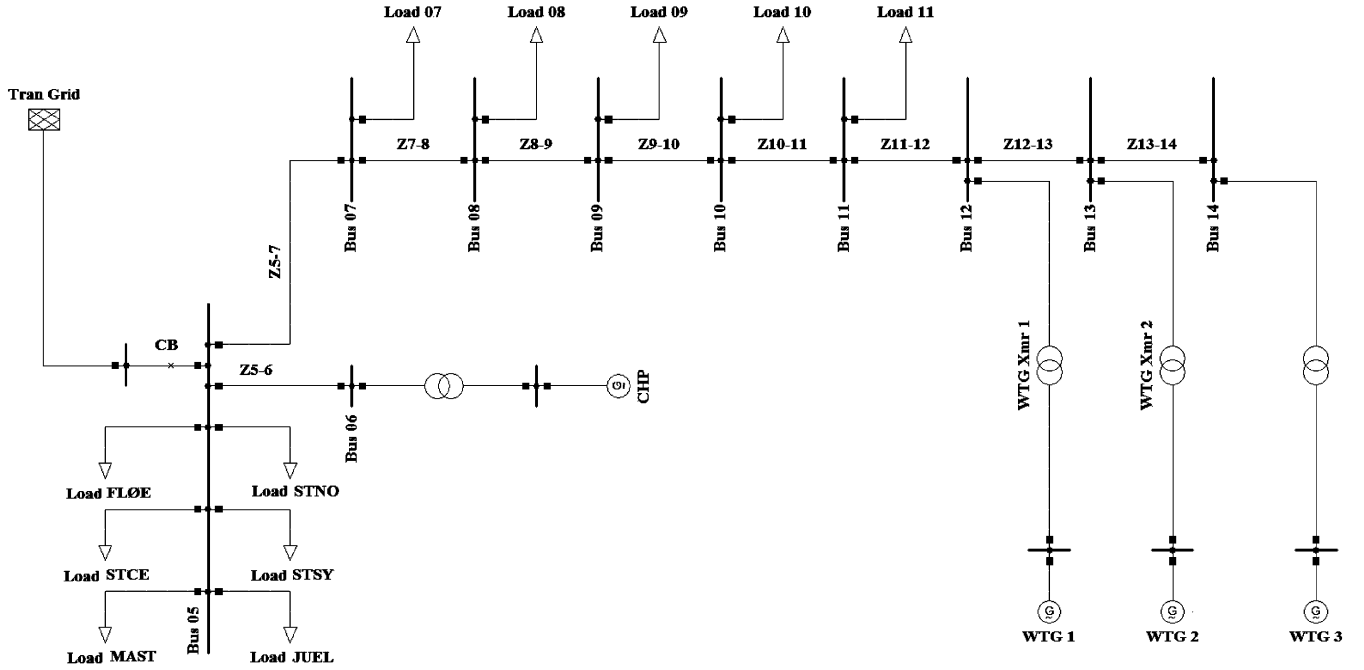


Fig. 3. Test system.

TABLE II
EXCITATION SYSTEM DATA

Parameters	Value
Measurement delay (s)	0
Controller minimum input (p.u.)	-7.5
Controller maximum input (p.u.)	9.35
Controller minimum output (p.u.)	-7.5
Controller maximum output (p.u.)	9.35
Filter delay time (s)	0.01
Filter derivative time constant (s)	0
Controller gain (p.u.)	250
Controller time constant (s)	0.01
Stabilization path gain (p.u.)	0.01
Stabilization path delay time (s)	1
Excitor current compensation factor (p.u.)	0

TABLE III
GOVERNOR SYSTEM DATA

Parameters	Value
Speed Droop (p.u.)	0.047
Controller Time Constant (s)	0.4
Actuator Time Constant (s)	0.1
Compressor Time Constant (s)	3.
Ambient Temperature Load Limit (p.u.)	0.909
Turbine Factor (p.u.)	1
Controller Minimum Output (p.u.)	0
Controller Maximum Output (p.u.)	1.2
Frictional losses factor (p.u.)	0
Turbine Rated Power (MW)	3.3

TABLE IV
WIND TURBINE AND DRIVE TRAIN DATA

Parameters	Value
Rotor Inertia (kg mm)	$4 \cdot 10^6$
Drive train Stiffness (Nm/rad)	8000
Drive train Damping (Nm/rad)	0
Rotor radius (m)	34

the CHP plant. An IEEE-type ST1 excitation system [18] and GAST model [19] are used to model the exciter and governor system in the CHP plant, respectively. The standard models, for exciter and governor, available in DIGSILENT, are used for the study. The data for exciter and governor systems is given in Tables II and III, respectively. For the purpose of this study, wind turbines are modeled as a two-mass system [20]. The data for the wind turbine system are given in Table IV. The data for the peak loads of December 2006 and January 2007 are given in Table V. F_{LL} and T are set as 0.99 p.u. and 10, respectively, for the test distribution system. In a real system, loads are always voltage and frequency dependent. However, it is very difficult to determine loads' voltage and frequency dependency. Hence, for simplicity, the loads are modeled as

$$P = P_0(1 + K_{pf}\Delta f + K_{pv}\Delta V)$$

$$Q = Q_0(1 + K_{qf}\Delta f + K_{qv}\Delta V)$$

where P and P_0 are the active power at a new voltage and frequency and base voltage and frequency, respectively; Q and Q_0 are the reactive power at new voltage and frequency, and base voltage and frequency, respectively; K_{fp} and K_{vp} are the coefficients of active load dependency on frequency and voltage, respectively; K_{fq} and K_{vq} are the coefficients of reactive load dependency on frequency and voltage, respectively; and Δf and ΔV are the deviations on frequency and voltage in per unit, respectively.

TABLE V
LOAD AND GENERATION DATA FOR THE TEST SYSTEM

Load	December 2006		January 2007	
	P (MW)	Q (MVar)	P (MW)	Q (MVar)
Load FLØE	1.888	0.453	2.109	0.576
Load JUEL	0.89	0.163	0.9	0.164
Load 07	0.4995	0.2054	0.4598	0.1341
Load 08	0.7868	0.3235	0.7243	0.2113
Load 09	0.1249	0.0514	0.115	0.0335
Load 10	0.1249	0.0514	0.115	0.0335
Load 11	0.1249	0.0514	0.115	0.0335
Load MAST	2.521	0.878	2.732	0.842
Load STCE	1.158	0.168	1.172	0.139
Load STNO	1.699	0.248	1.989	0.223
Load STSY	1.901	0.493	1.656	0.384

IV. SIMULATION RESULTS AND DISCUSSIONS

Peak demand from December 2006 is used to create the lookup table (Table I) and the proposed methodology is tested during the peak demand from January 2007. The CHP produced 9 MW during both times while WTGs produced 84 kW each when the system was islanded. The delay time is chosen as 80 ms, which is within the capabilities of currently available equipment. Various scenarios have been simulated to show the effectiveness of the proposed methodology. To simulate the worst possible case, loads are chosen to be highly frequency and voltage dependent. This will result in larger RoCoF and less load is shed at the first step, and the frequency will drop to lower values. Thus, K_{pf} , K_{pv} , K_{qf} , and K_{qv} are all chosen as 0.5. All of these events are simulated at time(t) = 0 seconds(s). The frequency drops to 49.535 Hz at 0.01 s, which gives the RoCoF of -46.28 Hz/s.

A. Case 1

In this scenario, smaller loads are willing to pay less so they are shed first. The ranking of loads and their willingness to pay is listed in Table I.

It can be observed from the lookup table that N is 3. Thus, the load shedding is initiated at 0.01 s and loads ranked 1–3 are shed at 0.09 s. The remaining loads will wait until $t = 0.09$ s before measuring the frequency and calculating RoCoF again. At 0.19 s, the RoCoF becomes negative for 10 continuous half cycles with the frequency below 0.99 p.u. and N becomes 4. Thus, load shedding of load ranked 4 is initiated at 0.19 s and it is shed at 0.27 s. Similarly, loads ranked 5, 6, and 7 are shed at 0.45 s, 0.63 s, and 0.81 s, respectively with the fulfillment of both load shedding criteria. No more loads are shed, and normal frequency is restored after some time. Fig. 4 shows the system frequency during islanding and load shedding for case 1. The frequency goes as low as 0.897 p.u. and it rises above 0.99 p.u. within 3.91 s. Fig. 5 shows the CHP turbine power for case 1.

B. Case 2

In a random case, it can be seen from the lookup table that the $\sum_{i=1}^N \text{RoCoF}_{Li}$ for the first load is -53.23 Hz/s, which is

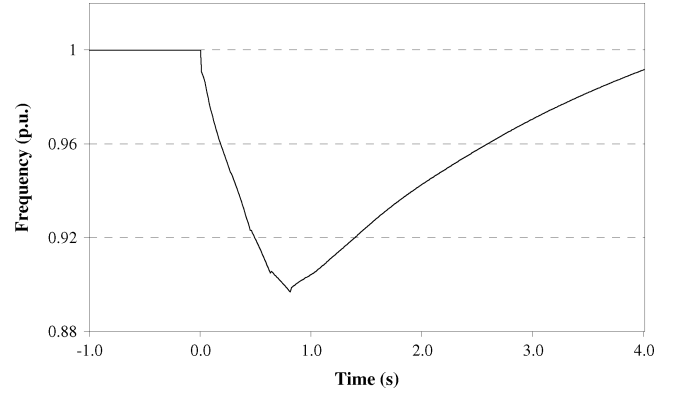


Fig. 4. System frequency during islanding and load shedding for case 1.

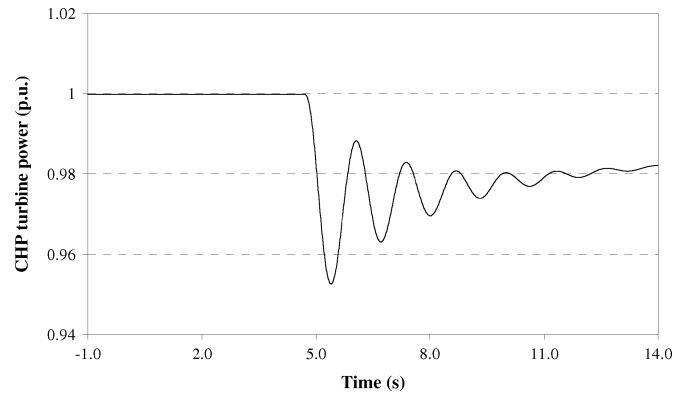


Fig. 5. CHP turbine power for case 1.

smaller than the RoCoF calculated when the system is islanded. But RoCoF is also smaller than RoCoF_{LLL} . Hence, load ranked 1 is shed at 0.09s. Now, the methodology will wait until the frequency goes down below 49.5 Hz (0.99 p.u.) and RoCoF becomes negative for 10 half cycles. The condition is fulfilled at time 0.20 s and, hence, load ranked 2 is shed at 0.28 s. The conditions are again fulfilled at 0.38 s and load ranked 3 is shed at 0.46 s. Fig. 6 shows the system frequency during islanding and load shedding for case 2. The frequency goes as low as 0.947 p.u. in this case and it rises above 0.99 p.u. within 1.85 s. Fig. 7 shows the CHP turbine power for case 2.

C. Case 3

In this case, load ranked 1 and 2 has a real power demand that almost matches the real power deficiency in the distribution system when it is islanded. Load ranked 3 and 4 are the two smallest loads.

Similar to case 2, first load shedding is initiated at 0.01 s and load ranked 1 is shed at 0.09 s. The second load shedding is initiated at 0.31 s and load ranked 2 is shed at 0.39 s. Similarly, loads ranked 3 and 4 are shed at 0.58 s and 0.77 s, respectively. Fig. 8 shows the system frequency during islanding and load shedding for case 3. The frequency goes as low as 0.969 p.u. in this case and it rises above 0.99 p.u. within 3.52 s. Fig. 9 shows the CHP turbine power for case 2.

Seven, three, and four loads are shed in cases 1, 2, and 3, respectively. Figs. 10–12 show the system frequency when one

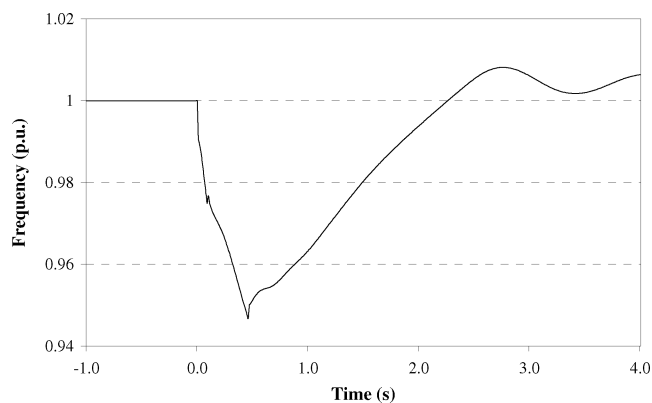


Fig. 6. System frequency during islanding and load shedding for case 2.

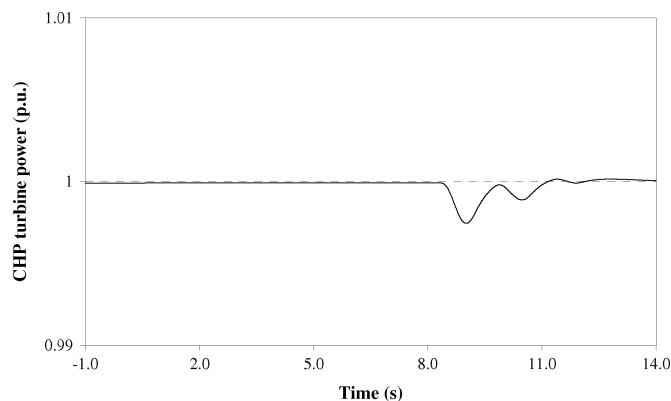


Fig. 9. CHP turbine power for case 3.

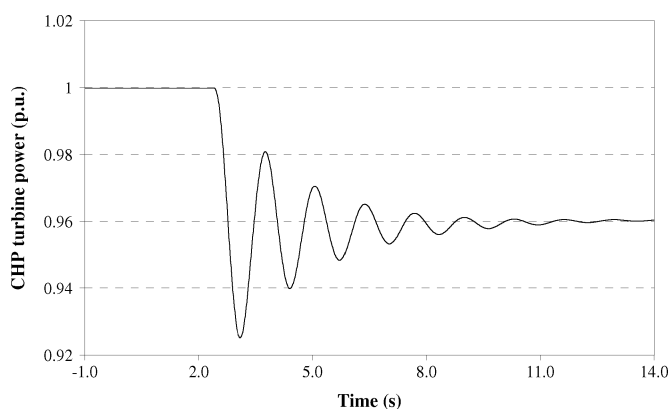


Fig. 7. CHP turbine power for case 2.

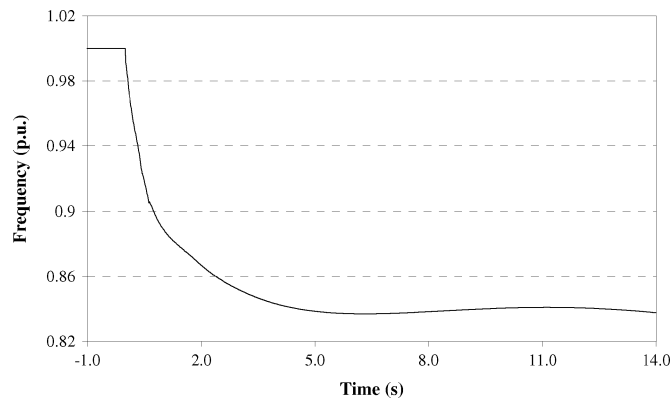


Fig. 10. System frequency during islanding and nonoptimal load shedding for case 1.

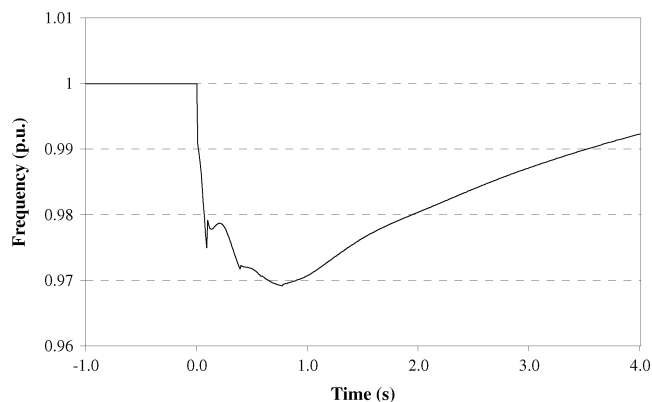


Fig. 8. System frequency during islanding and load shedding for case 3.

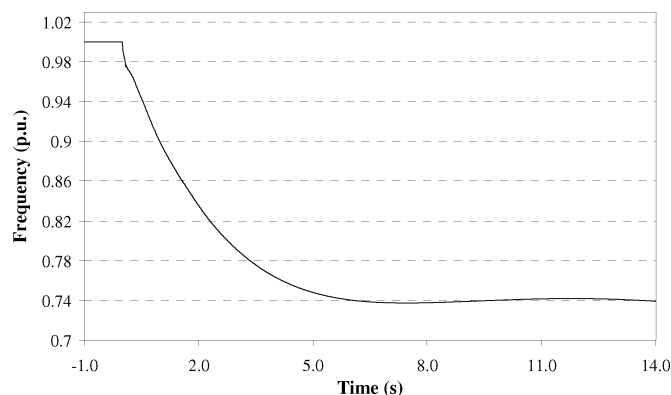


Fig. 11. System frequency during islanding and nonoptimal load shedding for case 2.

less load is shed, respectively, in cases 1, 2, and 3 with the shedding time of the shed loads remaining the same. This shows that the methodology sheds the optimal number of loads as the frequency does not rise to normal when one less load is shed. A total of 3.60 MW and 0.749 MVar, 3.76 MW and 0.64 MVar, and 3.422 MW and 1.043 MVar of loads are shed, respectively in cases 1, 2, and 3. The frequency comes back to normal ranges faster in case 2, which is expected with the highest amount of load shedding. The frequency reaches the lowest value in case 1, as smaller loads are shed in the beginning. This is, therefore, a worst-case scenario in terms of frequency dip. In case 3, the drop

of frequency is the lowest with the largest load shed at the first step. The total amount of load shed is also the optimal amount. The frequency thus takes a longer time to reach the normal operating range. However, the frequency is within the normal operation range of under/overfrequency relays. This is also true in other cases.

D. Case 4

In this case, K_{pf} , K_{pv} , K_{qf} , and K_{qv} are all chosen as 0. Thus, the loads have constant P and Q. A situation similar to

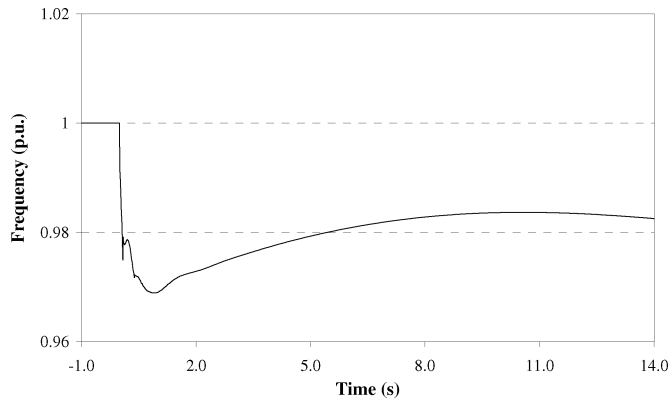


Fig. 12. System frequency during islanding and nonoptimal load shedding for case 3.

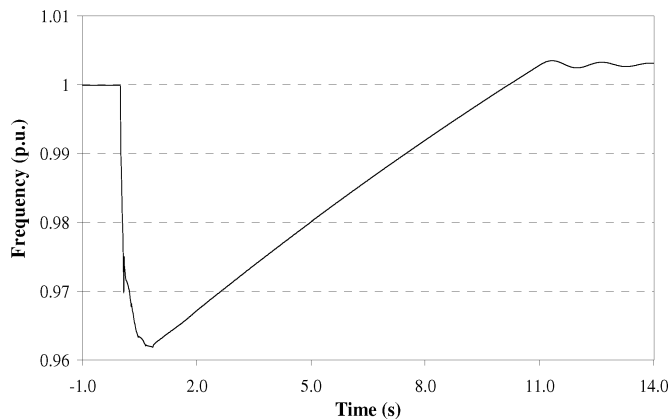


Fig. 13. System frequency during islanding and load shedding for case 4.

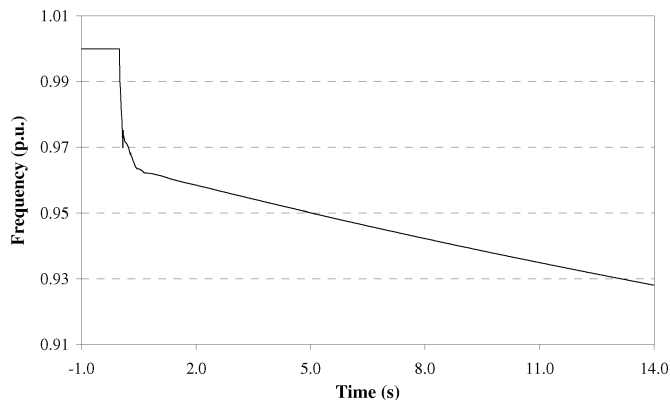


Fig. 14. System frequency during islanding and nonoptimal load shedding for case 4.

case 3 is simulated again. Now the frequency drops to 49.48 Hz at 0.1 s, giving an RoCoF of -52 Hz/s. Hence, only load ranked 1 is shed at 0.09 s. Loads ranked 2, 3, 4, and 5 are shed at 0.28 s, 0.47 s, 0.66 s, and 0.85 s, respectively, after fulfillment of the load shedding criteria. Fig. 13 shows the frequency of the system during islanding and load shedding. Fig. 14 shows the system frequency when one less load than optimal is shed. It clearly shows that the load shedding scheme sheds an optimal number of loads even when the loads do not have any dependency on voltage and frequency change.

V. CONCLUSION

A strategy to shed an optimal number of loads in a distribution system, when it is islanded and does not have sufficient generation to supply all of the loads, is presented to stabilize frequency. Frequency, rate of change of frequency, customers' willingness to pay, and loads histories have been used to develop the load shedding strategy, which is implemented in relays responsible for shedding loads.

The conventional load shedding strategy that is being successfully used in large power systems cannot be implemented in the islanded system because of the difference in the characteristics of the two systems. The load shedding strategy in the distribution system will not be based on the technical reason only but will depend on economic reasons as well. The proposed technique does not require communication between the components and real-time system data; rather, it uses loads histories to shed the loads automatically with declining frequency. The proposed underfrequency load shedding can stabilize the frequency of the distribution system with DGs when it is islanded by shedding an optimal number of loads.

REFERENCES

- [1] P. Djapic, C. Ramsay, D. Pudjianto, G. Strbac, J. Mutale, N. Jenkins, and R. Allan, "Taking an active approach," *IEEE Power Energy Mag.*, vol. 5, no. 4, pp. 68–77, Jul./Aug. 2007.
- [2] *Recommended Practice for Utility Interconnected Photovoltaic (PV) Systems*, IEEE Std. 929-2000, 2000.
- [3] *IEEE Standard for Interconnecting Distributed Resources Into Electric Power Systems*, IEEE Std. 1547TM, Jun. 2003.
- [4] P. G. Harrison, "Considerations when planning a load-shedding programme," *Brown Bovcri Rev.*, no. 10, pp. 593–598, Sep. 1988.
- [5] S. A. Nirenberg and D. A. McInnis, "Fast acting load shedding," *IEEE Trans. Power Syst.*, vol. 7, no. 2, pp. 873–877, May 1992.
- [6] M. Parniani and A. Nasri, "SCADA based under frequency load shedding integrated with rate of frequency decline," in *IEEE Power Eng. Soc. General Meeting 2006*, Jun. 2006. [Online]. Available: <http://ieeexplore.ieee.org/stamp/stamp.jsp?tp=&arnumber=1709594&isnumber=36065>
- [7] J. G. Thompson and B. Fox, "Adaptive load shedding for isolated power systems," *Proc. Inst. Elect. Eng., Gen., Transm. Distrib.*, vol. 141, no. 5, pp. 491–496, Sep. 1994.
- [8] X. Xiong and W. Li, "A new under-frequency load shedding scheme considering load frequency characteristics," in *Proc. Int. Conf. Power System Technology*, Oct. 2006, pp. 1–4.
- [9] V. N. Chuvychin, N. S. Gurov, S. S. Venkata, and R. E. Brown, "An adaptive approach to load shedding and spinning reserve control during under-frequency conditions," *IEEE Trans. Power Syst.*, vol. 11, no. 4, pp. 1805–1810, Nov. 1996.
- [10] L. Zhang and J. Zhong, "UFLS design by using f and integrating df/dt ," in *Proc. IEEE Power Eng. Soc. Power Systems Conf. Expo.*, 2006, pp. 1840–1844.
- [11] P. M. Anderson and M. Mirheydar, "An adaptive method for setting underfrequency load shedding relays," *IEEE Trans. Power Syst.*, vol. 7, no. 2, pp. 647–655, May 1992.
- [12] S. J. Huang and C. C. Huang, "An adaptive load shedding method with time-based design for isolated power systems," *Int. J. Elect. Power Energy Syst.*, vol. 22, pp. 51–58, Jan. 2000.
- [13] D. Prasetijo, W. R. Lachs, and D. Sutanto, "A new load shedding scheme for limiting underfrequency," *IEEE Trans. Power Syst.*, vol. 9, no. 3, pp. 1371–1378, Aug. 1994.
- [14] V. V. Terzija, "Adaptive under-frequency load shedding based on the magnitude of the disturbance estimation," *IEEE Trans. Power Syst.*, vol. 21, no. 3, pp. 1260–1266, Aug. 2006.
- [15] M. H. Purnomo, C. A. Patria, C. A. , and E. Purwanto, "Adaptive load shedding of the power system based on neural network," in *Proc. IEEE Region 10 Conf. Computers, Communications, Control Power Eng.*, Oct. 2002, vol. 3, pp. 1778–1781.

- [16] F. Carlsson and P. Martinsson, "Willingness to pay among Swedish households to avoid power outages—A random parameter tobit model approach," Working Papers in Economics 154 Göteborg Univ., Dept. Econom., Dec. 2004. [Online]. Available: <http://hdl.handle.net/2077/19626>
- [17] P. Mahat, Z. Chen, and B. Bak-Jensen, "A hybrid islanding detection technique using average rate of voltage change and real power shift," *IEEE Trans. Power Del.*, vol. 24, no. 2, pp. 764–771, Apr. 2009.
- [18] *IEEE Recommended Practice for Excitation System Models for Power System Stability Studies*. New York: IEEE, 1992.
- [19] Program Operation Manual, Power Technologies, Inc. New York, Power System Simulator—PSS/E.
- [20] S. Santoso and H. T. Le, "Fundamental time-domain wind turbine models for wind power studies," *Renew. Energy*, vol. 32, no. 14, pp. 2436–2452, Nov. 2007.



Pukar Mahat (S'08) received the B.Eng. degree in electrical and electronic engineering and the M.Eng. degree in electrical power system management from Kathmandu University, Dhulikhel, Nepal, and Asian Institute of Technology, Bangkok, Thailand, respectively, and is currently pursuing the Ph.D. degree in electrical and electronics engineering at the Institute of Energy Technology, Aalborg University, Aalborg, Denmark.

He was a Research Associate with the Asian Institute of Technology, Thailand. His research interests include distributed generation, wind power generation, and distribution system planning. He is a Certified Engineer in Nepal.



Zhe Chen (M'95–SM'98) received the B.Eng. degree in electrical and electronics engineering and the M.Sc. degree in power system automation and control from the Northeast China Institute of Electric Power Engineering, Jilin City, China, and the Ph.D. degree in power electronics and control from the University of Durham, Durham, U.K.

He was a Lecturer and then a Senior Lecturer with De Montfort University, U.K. Since 2002, he has been a Research Professor and is currently a Professor with the Institute of Energy Technology,

Aalborg University, Aalborg, Denmark. He is the Coordinator of the Wind Power System Research Program at the Institute of Energy Technology at Aalborg University. His background includes power systems, power electronics, and electric machines. His main primary research areas are wind energy and modern power systems. He has more than 170 publications in his technical field.

Dr. Chen is an Associate Editor (Renewable Energy) of the IEEE TRANSACTIONS ON POWER ELECTRONICS and Guest Editor of the IEEE TRANSACTIONS ON POWER ELECTRONICS Special Issue on Power Electronics for Wind Energy Conversion. He is a member of the Institution of Engineering and Technology (London, U.K.) and a Chartered Engineer in the U.K.



Birgitte Bak-Jensen (M'88) received the M.Sc. degree in electrical engineering and the Ph.D. degree in "modeling of high voltage components" from the Institute of Energy Technology, Aalborg University, Aalborg, Denmark, in 1985 and 1992, respectively.

From 1986 to 1988, she was an Electrical Design Engineer with Electrolux Elmotor A/S, Aalborg, Denmark. She is an Associate Professor in the Institute of Energy Technology, Aalborg University, where she has been since 1988. Her fields of interest are modeling and diagnosis of electrical components

as well as power quality and stability in power systems. Over the last few years, the integration of dispersed generation to the network grid has become one of her main fields, where she has participated in many projects concerning wind turbines and their connection to the grid.